Postnatal Expansion, Maturation and Functionality of MR1T Cells in Humans

Gwendolyn M. Swarbrick[1,4¶*], Anele Gela[5¶], Meghan E. Cansler[1], Megan D. Null[1], Rowan B. Duncan[1], Elisa Nemes[5], Muki Shey[5, 6], Mary Nsereko[7], Harriet Mayanja-Kizza[7, 8], Sarah Kiguli[7, 9], Jeffrey Koh[3], Willem A. Hanekom[5], Mark Hatherill[5], Christina Lancioni[1], David M. Lewinsohn[2, 4], Thomas J. Scriba[5&], Deborah A. Lewinsohn[1&]

[1]Division of Infectious Diseases, Department of Pediatrics, Oregon Health & Science University, Portland, Oregon, USA

[2]Division of Pulmonary and Critical Care Medicine, Department of Medicine, Oregon Health & Science University, Portland, Oregon, USA

[3]Department of Anesthesiology and Perioperative Medicine, Oregon Health & Science University, Portland, Oregon, USA

[4]Portland Veterans Administration Healthcare System, Portland, Oregon, USA

[5]South African Tuberculosis Vaccine Initiative, Institute of Infectious Disease and Molecular Medicine and Division of Immunology, Department of Pathology, University of Cape Town, Cape Town, South Africa

[6]Department of Medicine & Wellcome Centre for Infectious Disease Research in Africa (CIDRI-Africa), Institute of Infectious Disease and Molecular Medicine, University of Cape Town, South Africa

[7]Uganda-CWRU Research Collaboration, Kampala, Uganda.

[8]Dept of Medicine, Makerere University, Kampala, Uganda.

[9]Dept of Paediatrics, Makerere University, Kampala, Uganda.

*Correspondence
Gwendolyn Swarbrick
swarbric@ohsu.edu

¶These authors contributed equally to this work.

&These authors are Joint Senior Authors.

Keywords: innate T cells, human mucosal immunology, MAIT cells, infant, tuberculosis.

Abstract

MR1-restricted T (MR1T) cells are defined by their recognition of metabolite antigens presented by the monomorphic MHC class 1-related molecule, MR1, the most highly conserved MHC class I related molecule in mammalian species. Mucosal-associated invariant T (MAIT) cells are the predominant subset of MR1T cells expressing an invariant TCR α-chain, TRAV1-2. These cells comprise a T cell subset that recognizes and mediates host immune responses to a broad array of microbial pathogens, including *Mycobacterium tuberculosis*. Here, we sought to characterize development of circulating human MR1T cells as defined by MR1-5-OP-RU tetramer labelling and of the TRAV1-2^{+} MAIT cells defined by expression of TRAV1-2 and high expression of CD26 and CD161 (TRAV1-2^{+}CD161^{++}CD26^{++} cells). We analysed postnatal expansion, maturation and functionality of peripheral blood MR1-5-OP-RU tetramer^{+} MR1T cells in cohorts from three different geographic settings with different tuberculosis (TB) vaccination practices, levels of exposure to and infection with *M. tuberculosis.* Early after birth, frequencies of MR1-5-OP-RU tetramer^{+} MR1T cells increased rapidly by several fold. This coincided with the transition from a predominantly CD4^{+} and TRAV1-2^{-} population in neonates, to a predominantly TRAV1-2^{+}CD161^{++}CD26^{++} CD8^{+} population. We also observed that tetramer^{+} MR1T cells that expressed TNF upon mycobacterial stimulation were very low in neonates, but increased ~10-fold in the first year of life. These functional MR1T cells in all age groups were MR1-5-OP-RU tetramer^{+}TRAV1-2^{+} and highly expressed CD161 and CD26, markers that appeared to signal phenotypic and functional maturation of this cell subset. This age-associated maturation was also marked by the loss of naïve T cell markers on tetramer^{+} TRAV1-2^{+} MR1T cells more rapidly than tetramer^{+}TRAV1-2^{-} MR1T cells and non-MR1T cells. These data suggest that neonates have infrequent populations of MR1T cells with diverse phenotypic attributes; and that exposure to the environment rapidly and preferentially expands the MR1-5-OP-RU tetramer^{+}TRAV1-2^{+} population of MR1T cells, which becomes the predominant population of functional MR1T cells early during childhood.

53 **Introduction**

54 MR1-restricted T (MR1T) cells are T-cells that display a highly restricted T-cell-receptor
55 (TCR) repertoire and exhibit innate-like functions similar to those described for NKT cells. MR1T
56 cells are defined by their recognition of metabolite antigens presented by the monomorphic MHC
57 class 1-related molecule, MR1, the most highly conserved MHC class I related molecule in
58 mammalian species (Harriff et al., 2018; Godfrey et al., 2019). The TRAV1-2^{+} MR1T cells are
59 known as Mucosal Associate Invariant T cells (MAIT) and this subset express an invariant TCR
60 α-chain (TRAV1.2-TRAJ33/20/12 in humans; TRAV1-TRAJ33 in mice) with a CDR3 of constant
61 length paired with a limited number of Vβ segments (Vβ2/13 in humans; Vβ6/8 in mice) (Treiner
62 et al., 2003; Martin et al., 2009; Reantragoon et al., 2013; Lepore et al., 2014). MR1T cells have
63 been defined by different methods. Prior to availability of the MR1 tetramer, MR1T cells were
64 phenotypically defined as the predominant MAIT cell subset, by expression of TRAV1-2 and high
65 level expression of CD161 (Walker et al., 2012; Fergusson et al., 2014; Sharma et al., 2015) and
66 CD26 (Sharma et al., 2015). Now MR1 tetramers can also be more broadly used to define MR1T
67 cells. More specifically, the MR1-5-OP-RU tetramer, while not universally staining all MR1T
68 cells, stains the vast majority of MR1 tetramer staining T cells and has been widely used to define
69 this cell population (reviewed in Godfrey et al., 2019). In peripheral blood of adults, populations
70 of MR1-5-OP-RU tetramer^{+} MR1T cells are highly concordant with populations of TRAV1-
71 2^{+}CD161^{++}CD26^{++} phenotypically defined MAIT cells (Meermeier et al., 2016). As we will show
72 in this paper, the MR1-5-OP-RU tetramer allows detection of a much broader repertoire of MR1T
73 cells that are not only restricted to TRAV1-2^{+} MAIT cells. Moreover, we show that in neonates,
74 MR1-5-OP-RU tetramer^{+} MR1T cells and TRAV1-2^{+}CD161^{++}CD26^{++} T cells are much less
75 concordant populations.

76 MR1T cell development is a stepwise process, with an intra-thymic selection followed by
77 peripheral expansion. Using the MR1-5-OP-RU tetramer, Koay *et al* reported a three-stage
78 development pathway for mouse and human MR1T cell populations, where three populations of
79 human MR1T precursors were defined based on differential expression of CD27 and CD161. The
80 initial two stages of MR1-5-OP-RU tetramer^{+}TRAV1-2^{+}CD161^{-} cells, which were either CD27^{-}
81 or CD27^{+}, occurred in the thymus and these cells were low in the periphery. The more mature
82 MR1-5-OP-RU tetramer^{+}TRAV1-2^{+}CD161^{+}CD27^{+} cells, designated as stage 3, have been shown
83 to represent only a small fraction of T cells in the thymus and neonates but form a more abundant
84 population in adult blood (Martin et al., 2009; Dusseaux et al., 2011; Koay et al., 2016). Studies
85 utilizing TRAV1-2 and high level CD161 expression (CD8^{+}TRAV1-2^{+}CD161^{++} cells) to define
86 MAIT cells, similarly demonstrated low numbers of these cells in the neonates, which expand
87 postnatally (Walker et al., 2012; Fergusson et al., 2014). Such studies indicate that MR1T cell
88 thymopoeisis is complemented by an important postnatal peripheral expansion and maturation,
89 which was recently shown to be dependent upon acquisition of the intestinal microbiome
90 (Constantinides et al., 2019; Legoux et al., 2019).

91 Studies that define MAIT cells by phenotypic characteristics or by MR1 5-OP-RU staining
92 demonstrate that these cells are activated via both TCR-dependent and TCR-independent
93 mechanisms. Regarding TCR-dependent activation, MAIT cells recognize microbial derived
94 riboflavin (Vitamin B2) biosynthesis intermediate derivatives, such as 5-OP-RU (5-(2-

95 oxopropylideneamino)-6-d-ribitylaminouracil) and a broad spectrum of microbes that synthesize
96 riboflavin, including *S. aureus, E. coli, and C. albicans* (Gold et al., 2010; Kjer-Nielsen et al.,
97 2012; Gold et al., 2013; Corbett et al., 2014; Meermeier et al., 2016). While 5-OP-RU was the first
98 activating MR1 ligand defined, several other ligands have subsequently been defined, including
99 additional riboflavin-derived ligands, and both stimulatory and inhibitory ligands (Eckle et al.,
100 2014; Gherardin et al., 2016; Meermeier et al., 2016; Harriff et al., 2018). In addition, cytokines,
101 primarily IL-12, IL-18, and IL-15, act synergistically to activate MAIT cells, both by lowering the
102 threshold of TCR activation (Ussher et al., 2014; Sattler et al., 2015; Slichter et al., 2016) and/or
103 inducing MR1-independent activation (Fergusson et al., 2014; Ussher et al., 2014; Sattler et al.,
104 2015; Slichter et al., 2016; van Wilgenburg et al., 2016; Suliman et al., 2019). These TCR-
105 independent activation mechanisms are hypothesized to explain how MAIT cells may participate
106 in host defense to viruses and bacteria that do not synthesize riboflavin (Ussher et al., 2014; van
107 Wilgenburg et al., 2016). Once activated, MAIT cells display immediate effector function by
108 secreting inflammatory cytokines and cytotoxic molecules, which can kill infected cells (Gold et
109 al., 2010; Dusseaux et al., 2011; Le Bourhis et al., 2013; Kurioka et al., 2015). In a mouse model
110 of pulmonary legionella infection, MAIT cells afforded enhanced protection in an MR1-dependent
111 manner, mediated by the effector molecules IFN-γ and GM-CSF (Wang et al., 2018). MAIT cells
112 have also been shown to facilitate control of *Klebsiella pneumoniae, Mycobacterium bovis* BCG,
113 and *Francicella tularensis* infections (Georgel et al., 2011; Meierovics et al., 2013; Sakala et al.,
114 2015; Meierovics and Cowley, 2016). Many of the bacterial pathogens that are important causes
115 of infant morbidity and mortality, including *S. aureus*, *S. pneumoniae*, and enteric pathogens (e.g.
116 *E. coli*, *Klebsiella*, *Salmonella*), are recognized by MAIT cells. Moreover, MAIT cells may
117 contribute to viral immunity and hence host defense to viral pneumonia, which represents the
118 major cause of morbidity and mortality worldwide (Zar and Ferkol, 2014). MAIT cells possess
119 immediate innate-like, effector functions, and can therefore mediate immune functions before
120 priming, clonal expansion and maturation of antigen-specific MHC-restricted T cells (Gold et al.,
121 2013; Hartmann et al., 2018; Godfrey et al., 2019). Therefore, MAIT cells could play an important
122 role in host defense to a variety of pathogens, especially in infancy.

123 MAIT cells are known to also recognize and respond to *Mycobacterium tuberculosis,* the
124 leading global cause of mortality from a single infectious agent. Infants and young children suffer
125 disproportionately from disseminated and severe forms of tuberculosis (TB) disease and are
126 significantly more susceptible to disease than adults (Marais et al., 2004a; Marais et al., 2004b;
127 Marais et al., 2006). Here, we sought to characterize development of MR1T cells (defined by MR1-
128 5-OP-RU-tetramer staining) by analyzing postnatal expansion, maturation and changes in
129 phenotype and functionality in humans. We compared MR1T cell development in cohorts from
130 three different settings with differing TB vaccination practices and levels of exposure and infection
131 with *M. tuberculosis.*

Results

Human participants

We enrolled nine cohorts across three different countries to study MR1T cell development (Table 1). The cohorts in South Africa (SA) were neonates (cord blood, *n* = 10), infants (aged 10 weeks, BCG vaccinated at birth, *n* = 10) and adolescents [aged 14-18 years, BCG vaccinated at birth, QuantiFERON-TB Gold (QFT)-negative, *n* = 10]. The cohorts enrolled in the United States (US) were neonates (cord blood, *n* = 10), infants (aged 9-15 months, BCG unvaccinated, *n* = 10) and adults (aged 29-60 years, *n* = 10). The cohorts in Uganda (UG) were infants [2-24 months old, BCG vaccinated at birth +/-, tuberculin skin test (TST) +/-, *n* = 36], children (24 - 60 months, BCG vaccinated at birth +/-, TST +/-, *n* = 23) and adults (aged 18-60 years, BCG vaccinated at birth +/-, TST +/-, *n* = 91).

Frequencies of tetramer-defined MR1T cell and phenotypically defined MAIT cell populations increase with age irrespective of BCG vaccination

We defined MR1T cells as $CD3^+$ T cells positively labeled with the MR1-5-OP-RU tetramer. The MR1-6FP tetramer was as a negative control tetramer (Figure 1A). The MR1-6-FP tetramer stained a different population of cells than the MR1-5-OP-RU tetramer (Figure S1). In addition, MAIT cells, were defined phenotypically as $CD3^+$ T cells that co-expressed TRAV1-2 and high levels of CD161 ($CD161^{++}$) and CD26 ($CD26^{++}$) (Figure 1A and Figure S2). This phenotypic definition of MAIT cells is concordant with the vast majority of MR1-5-OP-RU tetramer-defined MR1T cells in adults (Sharma et al., 2015; Meermeier et al., 2016). We determined frequencies of MR1T cells and the phenotypically-defined MAIT cells in all cohorts (Figure 1B). Because of limited availability of the MR1-5-OP-RU tetramer, determination of MR1-5-OP-RU $tetramer^+$ MR1T cell frequencies in the Ugandan cohorts was performed on a subset of 10 donors (Figure 1B and Figure S3). In all cohorts, both MR1-5-OP-RU tetramer-defined MR1T cell and phenotypically-defined MAIT cell frequencies (Figure 1B) and absolute cell numbers (Figure S4) increased with age.

Tetramer-defined MR1T cell and phenotypically-defined MAIT cell populations are concordant in adults, adolescents and infants but discordant in neonates

We next determined the degree of concordance between tetramer-defined MR1T cell and phenotypically-defined MAIT cell populations. The majority of the phenotypically-defined MAIT cell population (TRAV1-$2^+CD161^{++}CD26^{++}$ cells) also stained with the MR1-5-OP-RU tetramer in infants, adolescents and adults, demonstrating high concordance between tetramer-defined MR1T cells and phenotypically-defined MAIT cells in these cohorts. (Figure 1C). However, in cord blood from both SA and US neonates, these two populations were discordant as the minority of TRAV1-2^+ $CD161^{++}CD26^{++}$ MAIT cells also stained with the MR1T tetramer (Figure 1C and Figure S5).

The MR1-5-OP-RU $tetramer^+$ subset of phenotypically-defined MAIT cells contain the functional population

To investigate whether MR1-5-OP-RU tetramer-defined MR1T cells and phenotypically-defined MAIT cells have different functional capacity, we measured TNF expression in the US cohort by intracellular cytokine staining (ICS) and flow cytometry following incubation with *M.*

173 *smegmatis*-infected A549 cells. Among all phenotypically defined TRAV1-2^{+}CD161^{++}CD26^{++}
174 MAIT cells, only the MR1-5-OP-RU tetramer^{+} subset expressed TNF; MR1-5-OP-RU tetramer-
175 negative cells, by contrast, did not appear to respond to *M. smegmatis* stimulation (Figure 2).
176 Because of this result, we focused on the functional, CD3^{+} MR1-5-OP-RU tetramer^{+} MR1T cells
177 for subsequent experiments.

178 **Neonates have higher proportions of CD4^{+} and TRAV1-2^{-} MR1T populations compared to**
179 **infants, adolescents and adults**

180 To explore the diversity of MR1T cells and how this may change during early development,
181 we applied the dimensionality reduction method, t-distributed stochastic neighbor embedding
182 (tSNE), on MR1-5-OP-RU tetramer^{+} MR1T cells. Five discrete phenotypic MR1T cell clusters
183 were identified in both the SA and US cohorts (Figure 3A-D), the relative proportions of which
184 varied with age (Figure 3B and D). Specifically, the CD4^{+} (Clusters 3 and 4) and TRAV1-2^{-}CD26^{-}
185 CD161^{-} (Clusters 1, 2 and 3) MR1T cell clusters predominated in neonates, while CD4^{-}CD8$^{+/-}$
186 TRAV1-2^{+}CD26^{+}CD161^{+} cluster (Cluster 5) was predominant in infant, adolescent, and adult
187 cohorts from both the US and SA (Figure 3B and D). Relative proportions of MR1T cell clusters
188 in 10 week old (SA) and 12 month old (US) infants were more similar to those in adults and
189 adolescents than to those in neonates, consistent with the hypothesis that MR1T cells expand
190 rapidly upon exposure to MR1T cell antigens (Figure 3E and F). It was also noteworthy that CD4^{-}
191 CD8$^{+/-}$TRAV1-2^{+}CD161^{+}CD26^{+} MR1T cells that fell into cluster 5 comprised a much lower
192 percentage of the MR1Ts in cord blood, while forming the dominant phenotype in 12-month-old
193 (US) infants. In the 10 week old (SA) infants, this cluster had started to appear but was not yet
194 "fully developed", suggesting that the transition from a predominantly CD4^{+} and TRAV1-
195 2^{-} population in neonates, to a predominantly TRAV1-2^{+}CD161^{++}CD26^{++} CD8^{+} population occurs
196 during the first months of life. We also note that in the US cohort only there is a population that is
197 positive for all markers (Cluster 6) that is present at low frequency in all ages.

198 **MR1T cells become more functional with age**

199 Next, we explored how tetramer-defined MR1T cells developed functionally with age in
200 the US cohort by tracking the TNF-expressing population following *M. smegmatis* or
201 PMA/Ionomycin stimulation. TNF-expressing tetramer^{+} MR1T cells in neonates were present at
202 very low frequencies (Figure 2B) and represented a much smaller proportion of the total tetramer^{+}
203 MR1T cell population than in infants and adults (Figure 4A and B). Proportions of tetramer^{+} MR1T
204 cells responding to either mycobacteria or PMA/Ionomycin were higher in infants than adults
205 ($p=0.0007$ and $p=0.0021$, respectively) or neonates ($p<0.0001$ for both stimulations). However,
206 because tetramer^{+} MR1T cell frequencies were higher in adults than infants (Figure 1B), overall
207 frequencies of TNF-producing MR1T cells were highest in adults. To explore the functional
208 capacity of MR1T cells relative to other T cell subsets within each cohort, we compared
209 proportions of TNF-expressing MR1T cells (CD3^{+}TCRγδ^{-}MR1-5-OP-RU^{+}) with TCRγδ T cells
210 (CD3^{+}TCRγδ^{+} MR1-5OPRU^{-}), CD4^{+} T cells (CD3^{+}TCRγδ^{-}MR1-5OPRU^{-}CD4^{+}) and CD8^{+} T cells
211 (CD3^{+}TCRγδ^{-}MR1-5OPRU^{-}CD4^{+}) after PMA/Ionomycin stimulation (Figure 4C). In neonates,
212 proportions of TNF-expressing MR1T cells were significantly higher than proportions of TCRγδ

213 T cells and $CD8^+$ T cells. In infants and adults, proportions of TNF-expressing MR1T cells were
214 significantly higher than $TCR\gamma\delta^+$, $CD4^+$ and $CD8^+$ T cells (Figure 4C).

215 **Functional $CD3^+$MR1-5-OP-RU^+ MR1T cells are TRAV1-2^+**

216 Next, we investigated TRAV1-2 expression among functional, TNF-expressing
217 $CD3^+$MR1-5-OP-RU^+ MR1T cells. Only TRAV1-2^+ MR1T cells produced TNF in response to
218 mycobacterial stimulation while TRAV1-2^- MR1T cells were not functional (Figure 4D). This
219 pattern was unique to mycobacterial stimulation since TNF-expressing TRAV1-2^- MR1T cells
220 were observed in response to PMA/Ionomycin stimulation, particularly in infants and adults
221 (Figure 4E). Interestingly, the vast majority of these functional, TNF-expressing TRAV1-2^+
222 MR1T cells also highly expressed the phenotypic markers, CD26 and CD161 (Figure 4F-G). Thus,
223 the $CD3^+$MR1-5-OP-RU^+TRAV1-$2^+CD161^{++}CD26^{++}$ MR1T cell population contains the
224 functional MR1T cells that respond to mycobacteria. The frequency of this population increases
225 very quickly with age.

226 **TRAV1-2^+ MR1T cells lose naïve markers more rapidly with age than TRAV1-2^- MR1T cells**
227 **or non-MR1T cells**

228 To characterize the development of MR1T cells further, we also measured expression of
229 CD27 and CD161, markers previously described to indicate MR1T cell maturation (Koay et al.,
230 2018), and CD45RA, CCR7, CD38 and CD56 on tetramer-defined MR1Ts (Figures 5-6). A
231 population of immature MR1T cells, defined as $CD27^+CD161^-$ cells, was observed in neonates but
232 not in infants and adults, as previously described (Koay et al., 2016). This was also reflected by
233 expression of the more traditional T cell maturation markers, CD45RA, CCR7 and CD38 (Figure
234 6 A, C, E). Most tetramer-defined MR1T cells in neonates displayed a $CD45RA^+CCR7^+CD38^+$
235 "naïve" phenotype, but this phenotype was lost more rapidly with age on TRAV1-2^+ MR1T cells
236 than on TRAV1-2^- MR1T cells or non-MR1T cells (Figure 6A-F). The inverse was true for the
237 activation marker, CD56, which was increased in neonatal, infant and adult TRAV1-2^+ tetramer-
238 defined MR1T cells compared to TRAV1-2^- tetramer-defined MR1T cells and non-MR1T cells
239 (Figure 6G-H). These results are consistent with our finding that TRAV1-2^+ tetramer-defined
240 MR1T cells display functional capacity in all age groups, even though they represent the minority
241 of neonatal MR1T cells.

242 **Discussion**

243 We characterized the development of MR1T cells during early childhood in three cohorts,
244 two from Africa and one in the USA, to elucidate phenotypic and functional changes that occur
245 after birth and during the first few years of life. A better understanding of MR1T cell development
246 is critical given the likely role of MR1T cells as innate-like effectors that act as key mediators of
247 immunity in newborns, who are at very high risk of infection, including *M. tuberculosis.* We found
248 that neonates had relatively low frequencies of MR1T cells with high phenotypic diversity, which
249 included considerable proportions of $CD4^+$ and TRAV1-2^- cells. These patterns changed as early
250 as 10 weeks after birth, and became more prominent at 1-2 years of age, adolescence and ultimately
251 by adulthood. This included higher frequencies of MR1T cells in peripheral blood, characterized
252 by a preferential expansion in TRAV1-2^+CD8^+ MR1T cells such that TRAV1-2^+CD8^+MR1T cells
253 constituted the vast majority of the $tetramer^+$ MR1T cell population. The development also
254 included changes in expression of maturation markers and MR1T cell effector function, since
255 MR1T cells from older individuals had lower expression of the naïve T cell markers, CD45RA,
256 CCR7 and CD38, and an increased ability to express TNF.

257 Our finding that MR1T cells are found at low frequency in cord blood and increase in
258 frequency with age confirms our previous observations, as well as those of others, who have
259 utilized either the MR1-5-OP-RU tetramer or phenotypic characterization of MAIT cells to
260 demonstrate the expansion of these cell populations from birth through adulthood (Martin et al.,
261 2009; Walker et al., 2012; Gold et al., 2013; Walker et al., 2014; Koay et al., 2016; Ben Youssef
262 et al., 2018; Gherardin et al., 2018). The very rapid changes in MR1T cells seen after birth are
263 striking and were clearly seen in both African and American settings. This finding rules out the
264 possibility that BCG substantially contributes to these changes, since BCG is not routinely
265 administered at birth in the USA and is consistent with the lack of differences in MAIT cell
266 magnitude or function between young infants either BCG immunized or unimmunized (Suliman
267 et al., 2019). Rather, it is more likely that changes occur upon the transition from the limited
268 microbial exposure in the womb to the postnatal environment, accompanied by the rapid
269 colonization of the gut microbiome. MR1T cells are absent in germ-free mice and depend on the
270 colonization of the gut microbiome with normal intestinal flora, which produce riboflavin (Le
271 Bourhis et al., 2013; Harriff et al., 2018; Legoux et al., 2019). We suggest that this colonization of
272 the gut microbiome is the driving force that accounts for the increase and phenotypic changes in
273 MR1T cells in blood after birth and the gain in functional capacity, though environmental exposure
274 and infection could also contribute.

275 While we confirm our previous work that phenotypic definition of MAIT cells accurately
276 identifies functional MR1T cells in adults, we find that there is a high level of discordance in
277 neonates in part due to MR1-5-OP-RU $tetramer^+$ cells that do not express TRAV1-2, and/or high
278 levels of CD161 or CD26. These cells are by definition MR1-restricted T cells as they bind the
279 MR1-5-OP-RU tetramer. However, these cells are poorly reactive to mycobacteria, suggesting
280 that they either recognize a different antigen or represent functionally immature MR1T cells. The
281 poor PMA/Ionomycin-induced TNF secretion of these cells supports the latter. However, because
282 our only measure of MR1T cell responses was TNF production, we may have failed to detect other
283 responses characterized by the production of alternative cytokines or cytolytic markers.

284 We also show that neonates possess MR1-5-OP-RU tetramer$^-$ cells that phenotypically
285 resemble MAIT cells (the discordant MR1-5-OP-RU tetramer$^-$ phenotypically defined TRAV1-
286 2$^+$CD161^{++}CD26^{++} MAIT cell population). As Fergusson *et al* suggested that distinct T subsets
287 that express CD161 share a common transcriptional profile characteristic of typical MR1T cells
288 (Fergusson et al., 2014), it is certainly possible that these CD161^{++} cells are MR1-restricted or
289 share common attributes with MR1T cells. Further characterization of this neonatal T cell
290 population is required to determine whether or not these cells are indeed MR1-restricted and if so,
291 if these cells are immature or recognize distinct microbes, or produce a different cytokine not
292 detected in our functional assay. Given that, in the mouse model, 5-OP-RU produced by the
293 microbiome is necessary and sufficient to drive the expansion of typical MR1T cells (Legoux et
294 al., 2019), it is perhaps expected that with age tetramer-positive MR1T TRAV1-2$^+$ cells would
295 quickly become the predominant MR1T cell population, while tetramer negative MR1T cells
296 might persist as a minority population of naïve T cells.

297 Consistent with our prior findings (Gold et al., 2013) and those of others (Walker et al.,
298 2012; Ben Youssef et al., 2018), our phenotypic analysis of MR1-5-OP-RU tetramer$^+$ cells in
299 neonates demonstrates that MR1T cells expressed a naïve cell surface phenotype
300 (CD45RA$^+$CCR7$^+$CD38$^+$) and included a prominent subset of CD4$^+$ cells. It is noteworthy that
301 these MR1T cells rapidly lost expression of CD45RA, CCR7 and CD38 and acquired a phenotype
302 consistent with those observed in antigen-experienced memory T cells much more rapidly than
303 other types of T cells (Chua et al., 2012; Tsukamoto et al., 2013; Lindestam Arlehamn et al., 2014).

304 While Koay *et al* showed the functional potential of neonatal MR1T cells that produced
305 TNF following stimulation with PMA/Ionomycin, we show for the first time the presence of
306 functional microbe-reactive MR1T cells in neonates, albeit at low frequency. Virtually all of the
307 mycobacteria-reactive TNF-producing MR1T cells were contained within the TRAV1-
308 2$^+$CD161^{++}CD26^{++} subset of 5-OP-RU tetramer$^+$ cells, which are also concordant with "Stage 3"
309 MR1T cells defined by Koay *et al*. Although the immature CD4$^+$, CD4-CD8- and/or TRAV1-2-
310 MR1T cells were maintained through to adulthood, we observed that CD8$^+$TRAV1-2$^+$ MR1T cells
311 expanded preferentially over TRAV1-2$^-$ MR1T cells. This expansion coincided with the
312 acquisition of high expression of CD26 and CD161 as markers of mature functional MR1 T cells.
313 Of note, studies evaluating the development of CD8$^+$CD161^{++} T cells in humans reported that a
314 lower proportion of this cell population expressed TRAV1-2 in neonates as compared to 2 year-
315 olds (Fergusson et al., 2014) and adults (Walker et al., 2012; Fergusson et al., 2014), and that in
316 adults, CD8$^+$CD161^{++} T cells producing IFN-γ in response to *E. coli* expressed TRAV1-2
317 (Fergusson et al., 2014). While these studies did not use the MR1 tetramer, these findings are
318 consistent with our results to the extent that the total CD8$^+$ CD161^{++} population reflected MR1T
319 cells. In addition, we show that the frequency of these functional mycobacterial-reactive MR1T
320 cells increases ~10-fold in the first year of life. A surprising finding was that given a comparable
321 stimulus (PMA/Ionomycin and *M. smegmatis*), the infant MR1T cells exhibited a higher functional
322 capacity than the adults. Interestingly, we demonstrated that relative to other T cell subsets, MR1T
323 cells had the highest capacity to secrete the pro-inflammatory cytokine, TNF, in infants. Thus,
324 MR1T cells may represent an important source of pro-inflammatory effectors in infants, who are
325 more vulnerable to serious bacterial infections in the first two years of life, relative to older
326 children and adults.

327 Regarding newborns, it is not known to what degree the naïve phenotype and low
328 functionality of MR1T cells contributes to the very high susceptibility to bacterial infection in the
329 first two months of life (Paul K Sue, 2018). Since MR1T cells recognize important childhood
330 bacterial pathogens, including *S. aureus, S. pneumoniae and enteric pathogens (e.g. E. coli,*
331 *Klebsiella, Salmonella species*, it is plausible that the low frequency of functional MR1T cells
332 during the neonatal period contributes to neonatal susceptibility to infection. At the very least, our
333 findings add to the well-described differences in adaptive and innate immunity between neonates
334 and adults (Paul K Sue, 2018).

335 With regard to *M. tuberculosis*, there is mounting evidence that supports an important host
336 defense role for MR1T cells, especially during early infection. Upon encounter with
337 mycobacterial-infected cells, MR1T cells produce pro-inflammatory cytokines such as IFN-γ and
338 TNF (Gold et al., 2010), known to be essential mediators to host defense against *M. tuberculosis*
339 (Lindestam Arlehamn et al., 2014). MR1-deficient mice control BCG less well than wild type
340 mice (Chua et al., 2012). In humans, MR1 polymorphisms are associated with susceptibility to TB
341 meningitis (Seshadri et al., 2017). It is tempting to speculate, in light of the high susceptibility of
342 infants to TB, and the phenotypic and functional attributes of MR1T cells we observed, that MR1T
343 cells contribute to control of early infection with *M. tuberculosis* through their early and robust
344 anti-mycobacterial response, particularly in the lung.

Methods

Study participants

University of Cape Town, Western Cape, South Africa. All participants were enrolled either at the South African Tuberculosis Vaccine Initiative Field Site, Well-Baby Clinics or Maternity Wards in the Worcester region, near Cape Town, South Africa. Pregnant mothers were enrolled for collection of cord blood immediately after childbirth by Cesarean section. Mothers who may have been exposed to *M. tuberculosis*, HIV infected, had any other acute or chronic disease, and receiving medication other than anesthetic given during delivery were excluded. Infants born to HIV negative mothers, and who had received BCG at birth, had no perinatal complications, or household contact with any person with TB, and did not have any acute or chronic disease were enrolled for collection of blood. Healthy adolescents of 12-18 years of age without evidence of latent Mtb infection as determined by positivity negativity for the Tuberculin Skin Test (<10mm) or QuantiFERON (<0.35IU/mL) were enrolled for blood collection. Heparinized blood was collected for cord blood mononuclear cell (CBMC) and peripheral blood mononuclear cells (PBMC) isolation by means of density gradient centrifugation.

Oregon Health and Science University, Portland, OR, USA. Umbilical cord blood was obtained from the placenta of uncomplicated term pregnancies after delivery into citrate CPT tubes (BD). Blood was processed per manufacturer's instructions within 24hr of collection, and resulting CBMC cryopreserved. Infants aged 1-24 months undergoing elective surgery at OHSU Doernbecher Children's Hospital were enrolled. Infants had not received BCG vaccination, which is not part of the childhood immunization series in the United States. Blood was drawn into citrate CPT tubes (BD) and processed per manufacturer's instructions to isolate PBMC within 24hr of collection, and PBMC subsequently cryopreserved. Adult PBMC were obtained by leukapheresis from healthy adult donors and cryopreserved. Adult participants lacked any detectable responses to *Mycobacterium tuberculosis* (Mtb) immunodominant antigens CFP-10 and ESAT-6 and therefore were assumed to be Mtb uninfected.

Makerere University, Kampala, Uganda. Children from age 2-60 months hospitalized with lower respiratory infection (LRTI) from etiologies other than TB were recruited from Mulago Hospital Paediatric Wards. All children were HIV-negative and had no known recent TB contacts. Children were reassessed two months following enrollment to establish vital status and ensure clinical improvement. Following completion of the study, data from all participating children was reviewed by study investigators (DAL, CLL, SK) to confirm diagnosis of non-TB LRTI. Blood was drawn into citrate CPT tubes (BD) and processed per manufacturer's instructions to isolate PBMC within 24hr of collection, and PBMC subsequently cryopreserved. Adult participants were recruited from the National TB Treatment Center at Mulago Hospital, hospital staff, and the community surrounding Kampala, Uganda, between 2001 and 2014. Participants were HIV uninfected and included individuals with (tuberculin skin test, TST ≥ 10) or without (TST < 10 mm) evidence of Mtb infection. All had the absence of signs or symptoms of TB (prolonged cough, hemoptysis, fever, weight loss, and night sweats). Heparinized blood was collected for PBMC isolation by means of density gradient centrifugation.

Study approvals

386 The studies of all participants were conducted in accordance with the World's Medical
387 Association's Declaration of Helsinki guidelines. The studies from the Western Cape, South Africa
388 were approved by the Human Research Ethics Committee (HREC) of the University of Cape
389 Town. Written informed consent was obtained from parents or legal guardians of adolescents and
390 infants. Adolescents also provided written informed assent. The Institutional Review Board of
391 Oregon Health & Science University (Portland, Oregon) approved this study of participants from
392 Portland, OR. Written, informed consent was obtained from all adult participants and from a parent
393 or legal guardian of infants before enrollment. For participants from Kampala, Uganda, the
394 National Council for Science and Technology, HIV/AIDS Research Committee in Uganda, the
395 Institutional Review Board of Oregon Health & Sciences University (Portland, OR) and the
396 Institutional Review Board of Makerere University (Kampala, Uganda) approved this study.
397 Written, informed consent was obtained from all adult participants and from a parent or legal
398 guardian of infants and children before enrollment.

399 **Infection of antigen presenting cells**

400 A549 cells (ATCC CCL-185) were used as stimulators for direct ex vivo determination of
401 mycobacterial-reactive T cells. *Mycobacterium smegmatis* (strain mc^2155, ATCC) was grown to
402 OD600 of 0.5 and frozen down. This was functionally titered in this assay to find the optimal
403 amount of *M. smegmatis* (4.13µl/ml) that elicited a strong response in an adult control donor but
404 did not reduce the viability of the antigen presenting cells. A549 cells were seeded in T25 flasks
405 at 1.25e6 in 7.5ml of antibiotic free media. After allowing cells to adhere for 3 hours, the flasks
406 were infected with 31µl of *M. smegmatis*. After 18 h, the cells were harvested and washed twice
407 in RPMI/10% human serum containing antibiotic (gentamicin) before being resuspended in
408 RPMI/10% human serum containing antibiotic (gentamicin).

409 **Flow cytometry assays**

410 To perform ICS, cryopreserved PBMC were thawed in the presence of DNAse,
411 resuspended, in 10% heat inactivated human serum with RPMI (Lonza) at a concentration of 2 x
412 10^7/ml. PBMC (2 x 10^6 cells/well) were stimulated with anti-CD28 (1 µg/ml) and anti-CD49d (1
413 µg/ml) (FastImmune, BD Biosciences) and 1e5 *M. smegmatis*-infected or uninfected A549 cells
414 in RPMI/10% Human Serum for 18 h at 37°C with 5% $C0_2$. During the last 12 h of this incubation,
415 Brefeldin-A (5 µg/ml) was added. PBMC incubated with uninfected A549 cells were used to assess
416 for background cytokine production. To determine the total functional capacity of T cells, PBMC
417 were incubated with uninfected A549 cells and PMA/Ionomycin (PMA, 20ng/ml, Sigma;
418 Ionomycin, 1µM, Sigma) for 3 hr. PBMC were then harvested and stained with MR1-5-OP-RU or
419 MR1-6FP tetramers (Corbett et al., 2014) (NIH Tetramer Core) at a 1:500 dilution for 45 minutes
420 at room temperature. All tetramers used were conjugated to R-phycoerythrin (PE) or Brilliant
421 Violet (BV) 421. After 45 minutes, an antibody cocktail containing LIVE/DEAD Fixable Dead
422 Cell Stain Kit (Thermo Fisher), and the surface antibodies listed in S1 Table were added for 30
423 minutes at 4°C. After washing, cells were fixed and permeabilized using Cytofix/Cytoperm (BD
424 Biosciences) per manufacturer's instructions. Cells were then stained for CD3 and TNF, then fixed
425 in 1% PFA. Acquisition was performed using a (Beckman Coulter) Cytoflex flow cytometer with

426 CytExpert software (BC). All flow cytometry data was analyzed using FlowJo software (TreeStar)
427 and Prism (Graphpad).

428 To perform cell surface staining for phenotyping MR1T cells, cryopreserved PBMC were
429 thawed as described above, and 1-2 x 10^6 PBMC were stained with MR1/5-OP-RU or MR1/6FP
430 tetramers at 1:500 for 45 minutes at room temperature. Cells were then subsequently stained with
431 an antibody cocktail containing LIVE/DEAD Fixable Dead Cell Stain Kit (Thermo Fisher), and
432 surface stained with the antibodies listed in S2-S4 Tables for 30 minutes at 4°C. Samples were
433 washed and fixed with 1% PFA. Acquisition of the US samples was performed using a Cytoflex
434 flow cytometer (Beckman) with CytExpert software (BC). For experiments with the Ugandan
435 samples, acquisition was performed on a BD LSRFortessa. For experiments performed at SATVI,
436 samples were acquired on a BD LSR-II flow cytometer configured with 4 lasers: solid state blue
437 (488nm; 100mW; 3 detectors), solid state violet (405nm; 25mW; 8 detectors), HeNe gas red
438 (635nm; 70mW; 3 detectors), and diode-pumped Coherent Compass yellow-green (532nm;
439 150mW; 8 detectors). Flow cytometric analysis was performed using FlowJo version 10.5.3
440 (Treestar, Ashland, OR, USA).

441 **Data analysis and Statistics**

442 Adjusted frequency (raw frequency of cytokine production following stimulation minus
443 the frequency of cytokine production in resting/unstimulated condition), was used to account for
444 the potential presence of background, or non-specific, responses. A positive cytokine response was
445 defined as the detection of at least 0.05% cytokine-positive T cells (following background
446 subtraction). Prism version 7 (GraphPad, La Jolla, CA, USA) was used for data analysis. A p-value
447 < 0.05 was considered as statistically significant.

448 To characterize phenotypic diversity within MR1T cell populations at the different ages
449 we performed t-Stochastic Neighbor Embedding (tSNE) on MR1-5-OP-RU tetramer$^+$ defined
450 CD3$^+$ T cells. Data from MR1-5-OP-RU tetramer$^+$ cells from all individuals across the age groups
451 were concatenated into a single FCS file to perform tSNE analysis in FlowJo. Equal event sampling
452 was not performed due to low events per individual in the cord blood and infant samples.
453 Clustering analysis was performed based on the expression of five surface markers (CD4, CD8,
454 TRAV1-2, CD26, and CD161). Parameter settings were fixed at 2000 iterations with a learning
455 rate (Eta) of 10 and perplexity 30, respectively (van der Maaten and Hinton, 2008).

456 **Conflict of Interest statement**

457 The authors declare that the research was conducted in the absence of any commercial or financial
458 relationships that could be construed as a potential conflict of interest.

Author Contributions

GMS, AG, DML, TJS and DAL contributed to the conception and/or design of the work. GMS and AG are joint first authors. TJS and DAL jointly supervised the work. MN, HMK, SK, JK, CL, EN, MS, WAH, MH and TJS contributed to clinical activities. EN, WAH, MH, DML, DAL and TJS raised grants to fund the research. GMS, AG, MEC, MDN, RBD, DML, TJS and DAL substantially contributed to the acquisition, analysis or interpretation of data and drafting of the manuscript. All authors substantially contributed to revising and critically reviewing the manuscript for important intellectual content. All authors approved the final version of this manuscript to be published and agree to be accountable for all aspects of the work.

Funding

This project has been funded in whole or in part with Federal funds from the National Institutes of Allergy and Infectious Diseases, National Institutes of Health, Department of Health and Human Services, under grant no R01 AI04229 and contract HHSN272200900053C.

Work at SATVI was supported by Aeras, the National Institutes of Health Grant R01-AI087915 and R01-AI065653 and the European and Developing Countries Clinical Trial Partnership. Anele Gela was supported by a Postdoctoral Fellowship from the Claude Leon Foundation.

The funders had no role in study design, data collection and analysis, decision to publish, or preparation of the manuscript.

Acknowledgments

We would like to thank the participants who gave time and dedication to this health research; W. Henry Boom, LaShaunda Malone and Keith Chervenak, Case Western Reserve University; and Erin Merrifield, Department of Pediatrics, OHSU, for their contributions to this study.

The MR1 tetramer technology was developed jointly by Dr. James McCluskey, Dr. Jamie Rossjohn, and Dr. David Fairlie, and the material was produced by the NIH Tetramer Core Facility as permitted to be distributed by the University of Melbourne.

This manuscript has been released as a pre-print at bioRxiv, (Swarbrick et al., 2019).

487 **References**

488 Ben Youssef, G., Tourret, M., Salou, M., Ghazarian, L., Houdouin, V., Mondot, S., et al. (2018).
489 Ontogeny of human mucosal-associated invariant T cells and related T cell subsets. *Journal*
490 *of Experimental Medicine* 215(2)**,** 459-479. doi: 10.1084/jem.20171739.
491 Chua, W.J., Truscott, S.M., Eickhoff, C.S., Blazevic, A., Hoft, D.F., and Hansen, T.H. (2012).
492 Polyclonal Mucosa-Associated Invariant T Cells Have Unique Innate Functions in
493 Bacterial Infection. *Infection and Immunity* 80(9)**,** 3256-3267. doi: 10.1128/Iai.00279-12.
494 Constantinides, M.G., Link, V.M., Tamoutounour, S., Wong, A.C., Perez-Chaparro, P.J., Han,
495 S.J., et al. (2019). MAIT cells are imprinted by the microbiota in early life and promote
496 tissue repair. *Science* 366(6464). doi: 10.1126/science.aax6624.
497 Corbett, A.J., Eckle, S.B.G., Birkinshaw, R.W., Liu, L.G., Patel, O., Mahony, J., et al. (2014).
498 T-cell activation by transitory neo-antigens derived from distinct microbial pathways.
499 *Nature* 509(7500)**,** 361-+. doi: 10.1038/nature13160.
500 Dusseaux, M., Martin, E., Serriari, N., Peguillet, I., Premel, V., Louis, D., et al. (2011). Human
501 MAIT cells are xenobiotic-resistant, tissue-targeted, CD161hi IL-17-secreting T cells.
502 *Blood* 117(4)**,** 1250-1259. doi: 10.1182/blood-2010-08-303339.
503 Eckle, S.B., Birkinshaw, R.W., Kostenko, L., Corbett, A.J., McWilliam, H.E., Reantragoon, R.,
504 et al. (2014). A molecular basis underpinning the T cell receptor heterogeneity of mucosal-
505 associated invariant T cells. *J Exp Med* 211(8)**,** 1585-1600. doi: 10.1084/jem.20140484.
506 Fergusson, J.R., Smith, K.E., Fleming, V.M., Rajoriya, N., Newell, E.W., Simmons, R., et al.
507 (2014). CD161 Defines a Transcriptional and Functional Phenotype across Distinct Human
508 T Cell Lineages. *Cell Reports* 9(3)**,** 1075-1088. doi: 10.1016/j.celrep.2014.09.045.
509 Georgel, P., Radosavljevic, M., Macquin, C., and Bahram, S. (2011). The non-conventional
510 MHC class I MR1 molecule controls infection by Klebsiella pneumoniae in mice. *Mol*
511 *Immunol* 48(5)**,** 769-775. doi: 10.1016/j.molimm.2010.12.002.
512 Gherardin, N.A., Keller, A.N., Woolley, R.E., Le Nours, J., Ritchie, D.S., Neeson, P.J., et al.
513 (2016). Diversity of T Cells Restricted by the MHC Class I-Related Molecule MR1
514 Facilitates Differential Antigen Recognition. *Immunity* 44(1)**,** 32-45. doi:
515 10.1016/j.immuni.2015.12.005.
516 Gherardin, N.A., Souter, M.N.T., Koay, H.F., Mangas, K.M., Seemann, T., Stinear, T.P., et al.
517 (2018). Human blood MAIT cell subsets defined using MR1 tetramers. *Immunology and*
518 *Cell Biology* 96(5)**,** 507-525. doi: 10.1111/imcb.12021.
519 Godfrey, D.I., Koay, H.F., McCluskey, J., and Gherardin, N.A. (2019). The biology and
520 functional importance of MAIT cells. *Nat Immunol* 20(9)**,** 1110-1128. doi:
521 10.1038/s41590-019-0444-8.
522 Gold, M.C., Cerri, S., Smyk-Pearson, S., Cansler, M.E., Vogt, T.M., Delepine, J., et al. (2010).
523 Human mucosal associated invariant T cells detect bacterially infected cells. *PLoS Biol*
524 8(6)**,** e1000407. doi: 10.1371/journal.pbio.1000407.
525 Gold, M.C., Eid, T., Smyk-Pearson, S., Eberling, Y., Swarbrick, G.M., Langley, S.M., et al.
526 (2013). Human thymic MR1-restricted MAIT cells are innate pathogen-reactive effectors
527 that adapt following thymic egress. *Mucosal Immunology* 6(1)**,** 35-44. doi:
528 10.1038/mi.2012.45.

Harriff, M.J., McMurtrey, C., Froyd, C.A., Jin, H.H., Cansler, M., Null, M., et al. (2018). MR1 displays the microbial metabolome driving selective MR1-restricted T cell receptor usage. *Science Immunology* 3(25). doi: UNSP eaao2556 10.1126/sciimmunol.aao2556.

Hartmann, N., Harriff, M.J., McMurtrey, C.P., Hildebrand, W.H., Lewinsohn, D.M., and Kronenberg, M. (2018). Role of MAIT cells in pulmonary bacterial infection. *Mol Immunol* 101**,** 155-159. doi: 10.1016/j.molimm.2018.06.270.

Kjer-Nielsen, L., Patel, O., Corbett, A.J., Le Nours, J., Meehan, B., Liu, L., et al. (2012). MR1 presents microbial vitamin B metabolites to MAIT cells. *Nature* 491(7426)**,** 717-723. doi: 10.1038/nature11605.

Koay, H.F., Gherardin, N.A., Enders, A., Loh, L., Mackay, L.K., Almeida, C.F., et al. (2016). A three-stage intrathymic development pathway for the mucosal-associated invariant T cell lineage. *Nature Immunology* 17(11)**,** 1300-1311. doi: 10.1038/ni.3565.

Koay, H.F., Godfrey, D.I., and Pellicci, D.G. (2018). Development of mucosal-associated invariant T cells. *Immunology and Cell Biology* 96(6)**,** 598-606. doi: 10.1111/imcb.12039.

Kurioka, A., Ussher, J.E., Cosgrove, C., Clough, C., Fergusson, J.R., Smith, K., et al. (2015). MAIT cells are licensed through granzyme exchange to kill bacterially sensitized targets. *Mucosal Immunology* 8(2)**,** 429-440. doi: 10.1038/mi.2014.81.

Le Bourhis, L., Dusseaux, M., Bohineust, A., Bessoles, S., Martin, E., Premel, V., et al. (2013). MAIT Cells Detect and Efficiently Lyse Bacterially-Infected Epithelial Cells. *Plos Pathogens* 9(10). doi: ARTN e1003681 10.1371/journal.ppat.1003681.

Legoux, F., Bellet, D., Daviaud, C., El Morr, Y., Darbois, A., Niort, K., et al. (2019). Microbial metabolites control the thymic development of mucosal-associated invariant T cells. *Science* 366(6464)**,** 494-499. doi: 10.1126/science.aaw2719.

Lepore, M., Kalinicenko, A., Colone, A., Paleja, B., Singhal, A., Tschumi, A., et al. (2014). Parallel T-cell cloning and deep sequencing of human MAIT cells reveal stable oligoclonal TCR beta repertoire. *Nature Communications* 5. doi: ARTN 3866 10.1038/ncomms4866.

Lindestam Arlehamn, C.S., Lewinsohn, D., Sette, A., and Lewinsohn, D. (2014). Antigens for CD4 and CD8 T cells in tuberculosis. *Cold Spring Harb Perspect Med* 4(7)**,** a018465. doi: 10.1101/cshperspect.a018465.

Marais, B.J., Gie, R.P., Schaaf, H.S., Hesseling, A.C., Enarson, D.A., and Beyers, N. (2006). The spectrum of disease in children treated for tuberculosis in a highly endemic area. *International Journal of Tuberculosis and Lung Disease* 10(7)**,** 732-738.

Marais, B.J., Gie, R.P., Schaaf, H.S., Hesseling, A.C., Obihara, C.C., Nelson, L.J., et al. (2004a). The clinical epidemiology of childhood pulmonary tuberculosis: a critical review of literature from the pre-chemotherapy era. *International Journal of Tuberculosis and Lung Disease* 8(3)**,** 278-285.

Marais, B.J., Gie, R.R., Schaaf, H.S., Hesseling, A.C., Obihara, C.C., Starke, J.J., et al. (2004b). The natural history of childhood intra-thoracic tuberculosis: a critical review of literature from the pre-chemotherapy era. *International Journal of Tuberculosis and Lung Disease* 8(4)**,** 392-402.

572 Martin, E., Treiner, E., Duban, L., Guerri, L., Laude, H., Toly, C., et al. (2009). Stepwise
573 Development of MAIT Cells in Mouse and Human. *Plos Biology* 7(3)**,** 525-536. doi:
574 ARTN e1000054
575 10.1371/journal.pbio.1000054.
576 Meermeier, E.W., Laugel, B.F., Sewell, A.K., Corbett, A.J., Rossjohn, J., McCluskey, J., et al.
577 (2016). Human TRAV1-2-negative MR1-restricted T cells detect S-pyogenes and
578 alternatives to MAIT riboflavin-based antigens. *Nature Communications* 7. doi: ARTN
579 12506
580 10.1038/ncomms12506.
581 Meierovics, A., Yankelevich, W.J.C., and Cowley, S.C. (2013). MAIT cells are critical for
582 optimal mucosal immune responses during in vivo pulmonary bacterial infection.
583 *Proceedings of the National Academy of Sciences of the United States of America* 110(33)**,**
584 E3119-E3128. doi: 10.1073/pnas.1302799110.
585 Meierovics, A.I., and Cowley, S.C. (2016). MAIT cells promote inflammatory monocyte
586 differentiation into dendritic cells during pulmonary intracellular infection. *Journal of*
587 *Experimental Medicine* 213(12)**,** 2793-2809. doi: 10.1084/jem.20160637.
588 Paul K Sue, M.M., and Maite de la Morena (2018). "Immunologic Development and
589 Susceptibility to Infection.," in *Principles and Practice of Pediatric Infectious Diseases.*
590 *5th ed.,* ed. G.C.P. S. Sarah Long, M. Fischer.: Elsevier), p85-92.
591 Reantragoon, R., Corbett, A.J., Sakala, I.G., Gherardin, N.A., Furness, J.B., Chen, Z.J., et al.
592 (2013). Antigen-loaded MR1 tetramers define T cell receptor heterogeneity in mucosal-
593 associated invariant T cells. *Journal of Experimental Medicine* 210(11)**,** 2305-2320. doi:
594 10.1084/jem.20130958.
595 Sakala, I.G., Kjer-Nielsen, L., Eickhoff, C.S., Wang, X., Blazevic, A., Liu, L., et al. (2015).
596 Functional Heterogeneity and Antimycobacterial Effects of Mouse Mucosal-Associated
597 Invariant T Cells Specific for Riboflavin Metabolites. *J Immunol* 195(2)**,** 587-601. doi:
598 10.4049/jimmunol.1402545.
599 Sattler, A., Dang-Heine, C., Reinke, P., and Babel, N. (2015). IL-15 dependent induction of IL-
600 18 secretion as a feedback mechanism controlling human MAIT-cell effector functions.
601 *Eur J Immunol* 45(8)**,** 2286-2298. doi: 10.1002/eji.201445313.
602 Seshadri, C., Thuong, N.T.T., Mai, N.T.H., Bang, N.D., Chau, T.T.H., Lewinsohn, D.M., et al.
603 (2017). A polymorphism in human MR1 is associated with mRNA expression and
604 susceptibility to tuberculosis. *Genes and Immunity* 18(1)**,** 8-14. doi: 10.1038/gene.2016.41.
605 Sharma, P.K., Wong, E.B., Napier, R.J., Bishai, W.R., Ndung'u, T., Kasprowicz, V.O., et al.
606 (2015). High expression of CD26 accurately identifies human bacteria-reactive MR1-
607 restricted MAIT cells. *Immunology* 145(3)**,** 443-453. doi: 10.1111/imm.12461.
608 Slichter, C.K., McDavid, A., Miller, H.W., Finak, G., Seymour, B.J., McNevin, J.P., et al. (2016).
609 Distinct activation thresholds of human conventional and innate-like memory T cells. *JCI*
610 *Insight* 1(8). doi: 10.1172/jci.insight.86292.
611 Suliman, S., Murphy, M., Musvosvi, M., Gela, A., Meermeier, E.W., Geldenhuys, H., et al.
612 (2019). MR1-Independent Activation of Human Mucosal-Associated Invariant T Cells by
613 Mycobacteria. *J Immunol* 203(11)**,** 2917-2927. doi: 10.4049/jimmunol.1900674.
614 Swarbrick, G.M., Gela, A., Cansler, M.E., Null, M.D., Duncan, R.B., Nemes, E., et al. (2019).
615 Postnatal expansion, maturation and functionality of MR1 T cells in humans. *bioRxiv***,**
616 2019.2012.2020.882746. doi: 10.1101/2019.12.20.882746.

617 Treiner, E., Duban, L., Bahram, S., Radosavljevic, M., Wanner, V., Tilloy, F., et al. (2003).
618 Selection of evolutionarily conserved mucosal-associated invariant T cells by MR1 (vol
619 422, pg 164, 2003). *Nature* 423(6943)**,** 1018-1018. doi: 10.1038/nature01700.
620 Tsukamoto, K., Deakin, J.E., Graves, J.A.M., and Hashimoto, K. (2013). Exceptionally high
621 conservation of the MHC class I-related gene, MR1, among mammals. *Immunogenetics*
622 65(2)**,** 115-124. doi: 10.1007/s00251-012-0666-5.
623 Ussher, J.E., Bilton, M., Attwod, E., Shadwell, J., Richardson, R., de Lara, C., et al. (2014).
624 CD161++ CD8+ T cells, including the MAIT cell subset, are specifically activated by IL-
625 12+IL-18 in a TCR-independent manner. *Eur J Immunol* 44(1)**,** 195-203. doi:
626 10.1002/eji.201343509.
627 van der Maaten, L., and Hinton, G. (2008). Visualizing Data using t-SNE. *Journal of Machine*
628 *Learning Research* 9**,** 2579-2605.
629 van Wilgenburg, B., Scherwitzl, I., Hutchinson, E.C., Leng, T., Kurioka, A., Kulicke, C., et al.
630 (2016). MAIT cells are activated during human viral infections. *Nat Commun* 7**,** 11653.
631 doi: 10.1038/ncomms11653.
632 Walker, L.J., Kang, Y.H., Smith, M.O., Tharmalingham, H., Ramamurthy, N., Fleming, V.M.,
633 et al. (2012). Human MAIT and CD8alphaalpha cells develop from a pool of type-17
634 precommitted CD8+ T cells. *Blood* 119(2)**,** 422-433. doi: 10.1182/blood-2011-05-353789.
635 Walker, L.J., Tharmalingam, H., and Klenerman, P. (2014). The Rise and Fall of MAIT Cells
636 with Age. *Scandinavian Journal of Immunology* 80(6)**,** 462-463. doi: 10.1111/sji.12237.
637 Wang, H.M., D'Souza, C., Lim, X.Y., Kostenko, L., Pediongco, T.J., Eckle, S.B.G., et al. (2018).
638 MAIT cells protect against pulmonary Legionella longbeachae infection. *Nature*
639 *Communications* 9. doi: ARTN 3350
640 10.1038/s41467-018-05202-8.
641 Zar, H.J., and Ferkol, T.W. (2014). The global burden of respiratory disease-impact on child
642 health. *Pediatr Pulmonol* 49(5)**,** 430-434. doi: 10.1002/ppul.23030.
643

644 **Figure Legends**

645 **Figure 1. Frequencies of tetramer-defined MR1T cell and phenotypically defined MAIT cell**
646 **populations in peripheral blood from individuals of different ages.** PBMC or CBMC were
647 stained with a live/dead discriminator, antibodies to CD3, CD4, CD8, TRAV1-2, CD26, CD161,
648 and either the MR1-5-OP-RU or MR1-6FP tetramers. Live, $CD3^+$ lymphocytes were gated and the
649 frequencies of MR1-5-OP-RU^+ or TRAV1-$2^+CD161^{++}CD26^{++}$ cells as a percentage of $CD3^+$
650 lymphocytes were determined (gating strategy in Figure S2). **A**. Flow cytometry plots showing
651 $CD3^+$ T cell staining with MR1-5-OP-RU tetramer, MR1-6FP tetramer, TRAV1-2 or
652 CD26/CD161 of samples from a representative US adult, infant and neonate. **B.** Frequencies of
653 tetramer-defined ($CD3^+$MR1-5-OP-RU^+) and phenotypically-defined ($CD3^+$TRAV1-2^+
654 $CD161^{++}CD26^{++}$) MAIT cells in neonates, 10 week-old infants and adolescents from South Africa,
655 neonates, 12 month-old infants and adults from the United States and infants (0-2 years old),
656 children (2-5 years old) and adults from Uganda (all cohorts, *n*=10). Mann-Whitney u-tests were
657 used to test differences between groups. Horizontal lines depict the median and the error bars the
658 95% confidence interval. **C.** Relative proportions of median phenotypically-defined
659 ($CD3^+$TRAV1-$2^+CD161^{++}CD26^{++}$) MAIT cells that are MR1-5-OP-RU^+ (Blue) and MR1-5-OP-
660 RU^- (Red) for each age group at each site.

661 **Figure 2. Functional analysis of MAIT cells in individuals of different ages.** PBMC or CBMC
662 from the US cohort were incubated overnight with *M. smegmatis*-infected A549 cells or uninfected
663 A549 cells and then stained with the MR1-5-OP-RU or MR1-6FP tetramers, followed by staining
664 with a live/dead discriminator and antibodies to TCRγδ, CD3, CD4, CD8, TRAV1-2, CD26 and
665 CD161. ICS was then performed and the cells stained for TNF. **A.** Dot plots showing representative
666 co-staining of live, $TCR\gamma\delta^-CD3^+$TRAV1-$2^+CD161^{++}CD26^{++}$ cells with MR1-5-OP-RU and TNF
667 in *M. smegmatis* stimulated or unstimulated samples. The gating strategy is in Figure S6. Examples
668 of the TNF response in a neonate, infant and adult are shown. **B.** Frequencies of phenotypically-
669 defined ($CD3^+$TRAV1-$2^+CD161^{++}CD26^{++}$) MAIT cells that are TNF^+MR1-5-OP-RU^+ or
670 TNF^+MR1-5-OP-RU^- are shown. Horizontal lines depict the median and the error bars the 95%
671 confidence interval. Wilcoxon-rank sum was used to test differences within the same cohort.

672 **Figure 3. Phenotypic diversity of MR1T cells in individuals of different ages.** t-Distributed
673 stochastic neighbor embedding (tSNE) plots showing MR1-5-OP-RU $tetramer^+CD3^+$ T cells
674 (gating strategy in Figure S2) from the South African (SA) or United States (US) cohorts (Table1).
675 Plots represent cells from 10 samples from each age group. **A.** and **C.** The five clusters identified
676 in both sites are shown in **A** (SA) and **C** (US). **B.** and **D.** Dot plots colored by the relative
677 expression level of each marker (CD4, CD8, TRAV1-2, CD161 or CD26) in tetramer-defined
678 MR1T cells for each age group in **B** (SA) and **D** (US). Red = highest expression, blue = lowest
679 expression. **E.** and **F.** The proportion of each cluster of tetramer-defined MR1T cells by age group
680 is shown in **E** (SA) and **F** (US). Horizontal lines depict the median and the error bars the 95%
681 confidence interval. Mann-Whitney u tests were used to test differences between groups.

682 **Figure 4. Phenotypic analysis of functional MR1T cells at different ages.** PBMC or CBMC
683 from the US cohort were incubated overnight with *M. smegmatis*-infected A549 cells, uninfected
684 A549 cells, or uninfected A549 cells and PMA/ionomycin. All cells were then stained with the

685 MR1-5-OP-RU or MR1-6FP tetramers, followed by a live/dead discriminator and antibodies to
686 TCRγδ, CD3, CD4, CD8, TRAV1-2, CD26 and CD161. ICS was then performed and the cells
687 stained for TNF. Live, TCRγδ$^-$CD3$^+$MR1-5-OP-RU$^+$ cells were gated and the TNF$^+$ percentage
688 determined in both the *M. smegmatis* stimulated and unstimulated conditions. The gating strategy
689 is shown in Figure S6. **A.** Dot plots showing TNF expression by live, TCRγδ$^-$MR1-5-OP-RU$^+$
690 CD3$^+$ cells in the same representative neonate, infant and adult as Figure 2A. **B.** Background
691 subtracted frequencies of TNF$^+$ MR1-5-OP-RU$^+$ CD3$^+$ cells in response to *M. smegmatis*-infected
692 A549 cells as a percentage of total MR1-5-OP-RU$^+$ CD3$^+$ cells are shown. Mann-Whitney u-tests
693 were used to test differences between groups. **C.** Background subtracted frequencies of TNF$^+$
694 cells to PMA/ionomycin among different T cell subpopulations, 1) MR1T cells (CD3$^+$TCRγδ$^-$
695 MR1-5-OP-RU$^+$ cells); 2) γδ T cells (CD3$^+$TCRγδ$^+$MR1-5-OP-RU$^-$ cells); 3) CD8$^+$ T cells
696 (CD3$^+$TCRγδ$^-$MR1-5-OP-RU$^-$CD8$^+$ cells); and 4) CD4$^+$ T cells (CD3$^+$TCRγδ$^-$MR1-5-OP-RU$^-$
697 CD4$^+$ cells). Wilcoxon-rank sum was used to test differences within the same cohort. **D.** and **E.**
698 Frequencies of TNF$^+$TRAV1-2$^+$ MR1-5-OP-RU$^+$ CD3$^+$ and TNF$^+$TRAV1-2$^-$ MR1-5-OP-RU$^+$
699 CD3$^+$ cells in response to *M. smegmatis* infected A549 cells (**D**) or PMA/ionomycin stimulation
700 (**E**) minus the background frequencies of TNF$^+$TRAV1-2$^+$/- MR1-5-OP-RU$^+$ CD3$^+$ cells.
701 Wilcoxon-rank sum was used to test differences within the same cohort. **F.** and **G.** Frequencies of
702 CD161^{++}CD26^{++} cells of the TNF$^+$TRAV1-2$^+$MR1-5-OP-RU$^+$CD3$^+$ cells in response to *M.*
703 *smegmatis* infected A549 cells (**F**) or PMA/ionomycin stimulation (**G**) are shown. The median and
704 95% confidence intervals are shown in each graph. When the 95% confidence intervals do not
705 overlap between conditions, those conditions are considered statistically significant.

706 **Figure 5. Analysis of MR1T cell development by measuring maturation markers.** PBMC or
707 CBMC from the US were stained as in Figure 1 with the addition of an antibody to CD27. Live,
708 CD3$^+$MR1-5-OP-RU$^+$ cells (gating strategy in Figure S2) were gated for the maturation pattern of
709 S1, S2 and S3 described in (Koay et al., 2016). S1 = CD161$^-$CD27$^-$, S2=CD161$^-$CD27$^+$,
710 S3=CD161$^+$CD27$^{+/-}$. **A.** Gating of MR1T cells for S1, S2 and S3 in a representative neonate, infant
711 and adult. **B.** Frequencies of S1, S2, and S3 MR1T cells as a percentage of CD3$^+$ MR1-5-OP-RU$^+$
712 cells are shown for U.S. neonates, infants and adults. Bars represent the median and the error bars
713 the 95% confidence interval.

714 **Figure 6. Comparative phenotypic analysis of MR1T and non-MR1T cells or TRAV1-2$^+$ and**
715 **TRAV1-2$^-$ MR1T cells at different ages.** PBMC or CBMC from the US were stained as in Figure
716 1 with the addition of antibodies to either CD45RA (**A, B**), CCR7 (**C, D**), CD38 (**E, F**) or CD56
717 (**G, H**). The gating strategy is shown in Figure S2 and examples of the staining of each marker is
718 shown in Figure S7. Frequencies of cells expressing each marker in non-MR1T cells (CD3$^+$MR1-
719 5-OP-RU$^-$) or MR1T cells (CD3$^+$MR1-5-OP-RU$^+$) in each age group (**A, C, E, G**). The frequency
720 of each marker expressed in TRAV1-2$^+$ or TRAV1-2$^-$ MR1T cells is shown in each age group (**B,**
721 **D, F, H**). The median and 95% confidence intervals are shown in each graph. When the 95%
722 confidence intervals do not overlap between conditions, those conditions are considered
723 statistically significant.

724 Tables

725 **Table 1. Study Participants**

Country	*Cohort*	*number*	*Age*	*BCG vaccination*	*QFT results*	*TST results*
South Africa	Neonates	10	0 (cord blood)	-	ND	ND
	Infants	10	10 weeks	100%	ND	ND
	Adolescents	10	14-18 years	100%	100% negative	ND
USA	Neonates	10	0 (cord blood)	-	ND	ND
	Infants	10	9-15 months	-	ND	ND
	Adults	10	29-60 years	-	ND*	ND*
Uganda	Infants	36	2-24 months	83% (n=30)	ND	36% (n=13)
	Children	23	24-60 months	78% (n=18)	ND	39% (n=9)
	Adults	91	18-60 years	+/-**	ND	51% (n=47)

726 ND = Not Done. *While QFT and TST were not performed, the infection status in Oregon is
727 likely to be negative based on epidemiology and results of an in-house ESAT-6/CFP-10 IFN-γ
728 ELISPOT assay. **This information is not known.

729

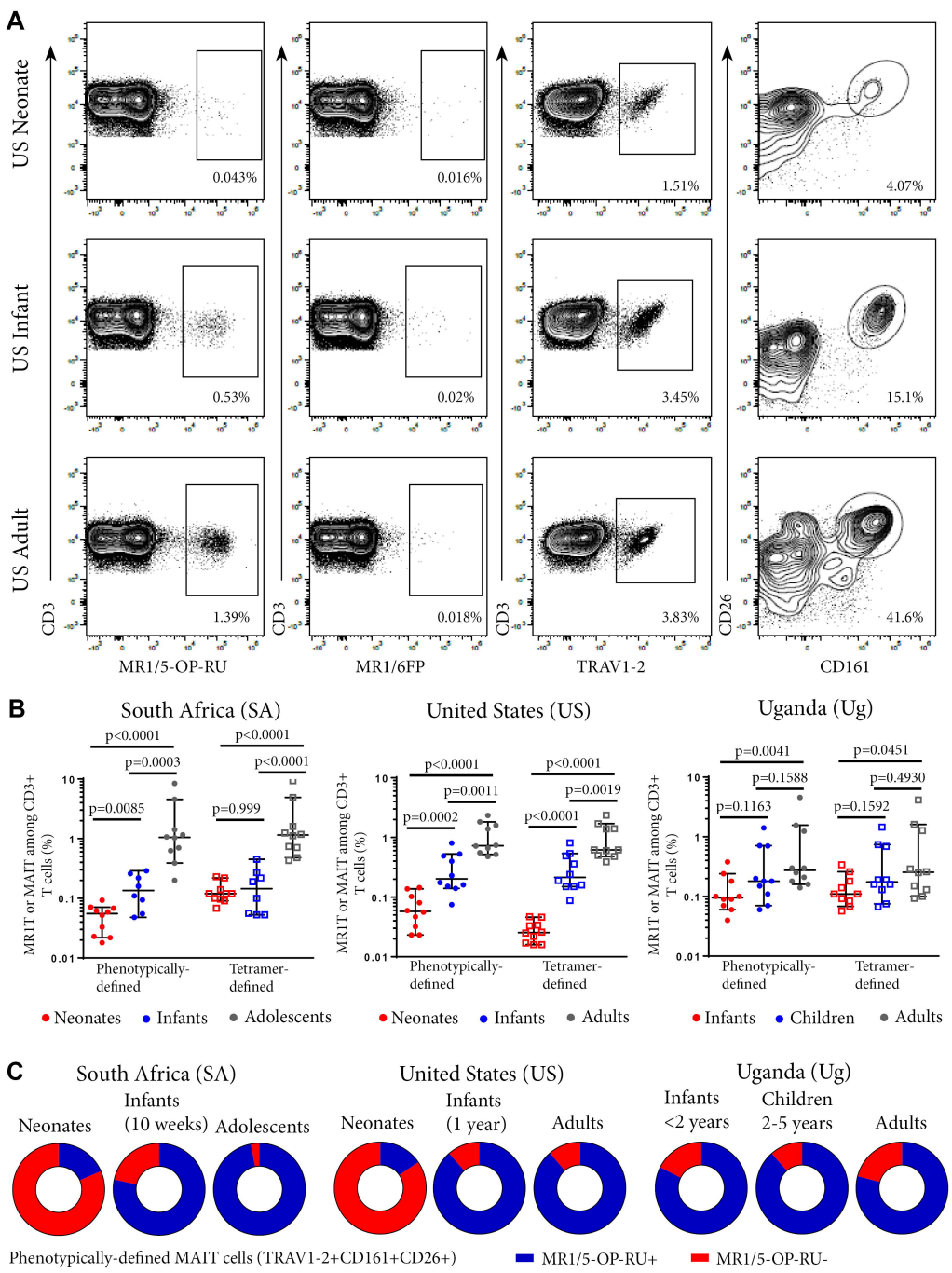
A
US Neonate
US Infant
US Adult
0.043%
0.016%
1.51%
4.07%
0.53%
0.02%
3.45%
15.1%
1.39%
0.018%
3.83%
41.6%
CD3
MR1/5-OP-RU
MR1/6FP
TRAV1-2
CD26
CD161
B
South Africa (SA)
United States (US)
Uganda (Ug)
MR1T or MAIT among CD3+ T cells (%)
p<0.0001
p=0.0003
p=0.0085
p<0.0001
p<0.0001
p=0.999
p<0.0001
p<0.0001
p=0.0011
p=0.0002
p<0.0001
p<0.0001
p=0.0019
p=0.0041
p=0.1588
p=0.1163
p=0.0451
p=0.4930
p=0.1592
Phenotypically-defined
Tetramer-defined
Neonates
Infants
Adolescents
Adults
Children
C
South Africa (SA)
Neonates
Infants (10 weeks)
Adolescents
United States (US)
Neonates
Infants (1 year)
Adults
Uganda (Ug)
Infants <2 years
Children 2-5 years
Adults
Phenotypically-defined MAIT cells (TRAV1-2+CD161+CD26+)
MR1/5-OP-RU+
MR1/5-OP-RU-

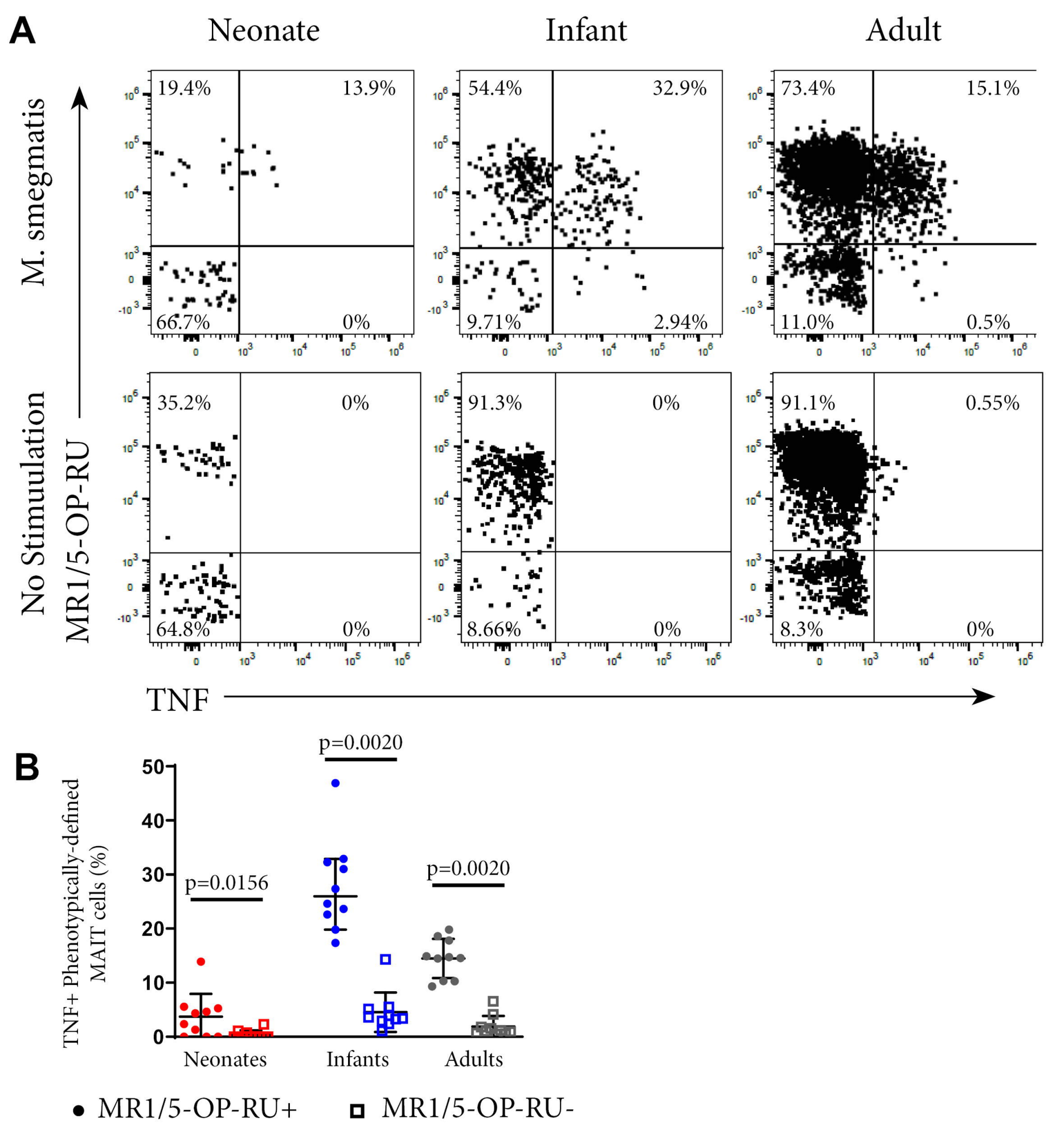
A
Neonate
Infant
Adult
M. smegmatis
No Stimulation
MR1/5-OP-RU
19.4%
13.9%
66.7%
0%
54.4%
32.9%
9.71%
2.94%
73.4%
15.1%
11.0%
0.5%
35.2%
0%
64.8%
0%
91.3%
0%
8.66%
0%
91.1%
0.55%
8.3%
0%
TNF
B
TNF+ Phenotypically-defined MAIT cells (%)
p=0.0156
p=0.0020
p=0.0020
Neonates
Infants
Adults
MR1/5-OP-RU+
MR1/5-OP-RU-

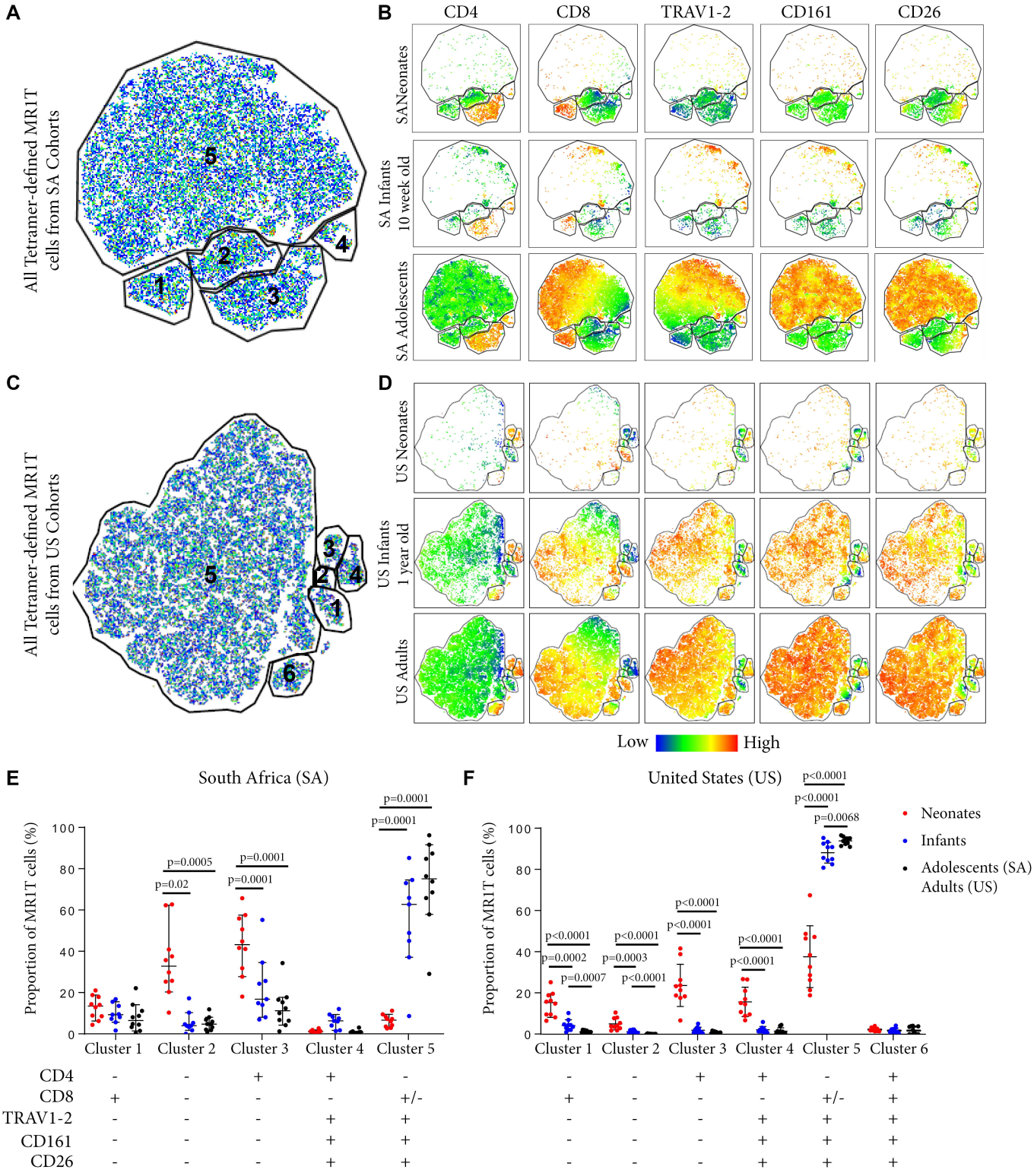
A
All Tetramer-defined MR1T cells from SA Cohorts
1
2
3
4
5
B
CD4
CD8
TRAV1-2
CD161
CD26
SANeonates
SA Infants 10 week old
SA Adolescents
C
All Tetramer-defined MR1T cells from US Cohorts
1
2
3
4
5
6
D
US Neonates
US Infants 1 year old
US Adults
Low
High
E
South Africa (SA)
Proportion of MR1T cells (%)
Cluster 1
Cluster 2
Cluster 3
Cluster 4
Cluster 5
p=0.02
p=0.0005
p=0.0001
p=0.0001
p=0.0001
p=0.0001
p=0.0001
F
United States (US)
Proportion of MR1T cells (%)
Cluster 1
Cluster 2
Cluster 3
Cluster 4
Cluster 5
Cluster 6
p<0.0001
p=0.0002
p=0.0007
p<0.0001
p=0.0003
p<0.0001
p<0.0001
p<0.0001
p<0.0001
p<0.0001
p<0.0001
p<0.0001
p=0.0068
Neonates
Infants
Adolescents (SA)
Adults (US)
CD4 - - + + - - - + + - +
CD8 + - - - +/- + - - - +/- +
TRAV1-2 - - - + + - - - + + +
CD161 - - - + + - - - + + +
CD26 - - - + + - - - + + +

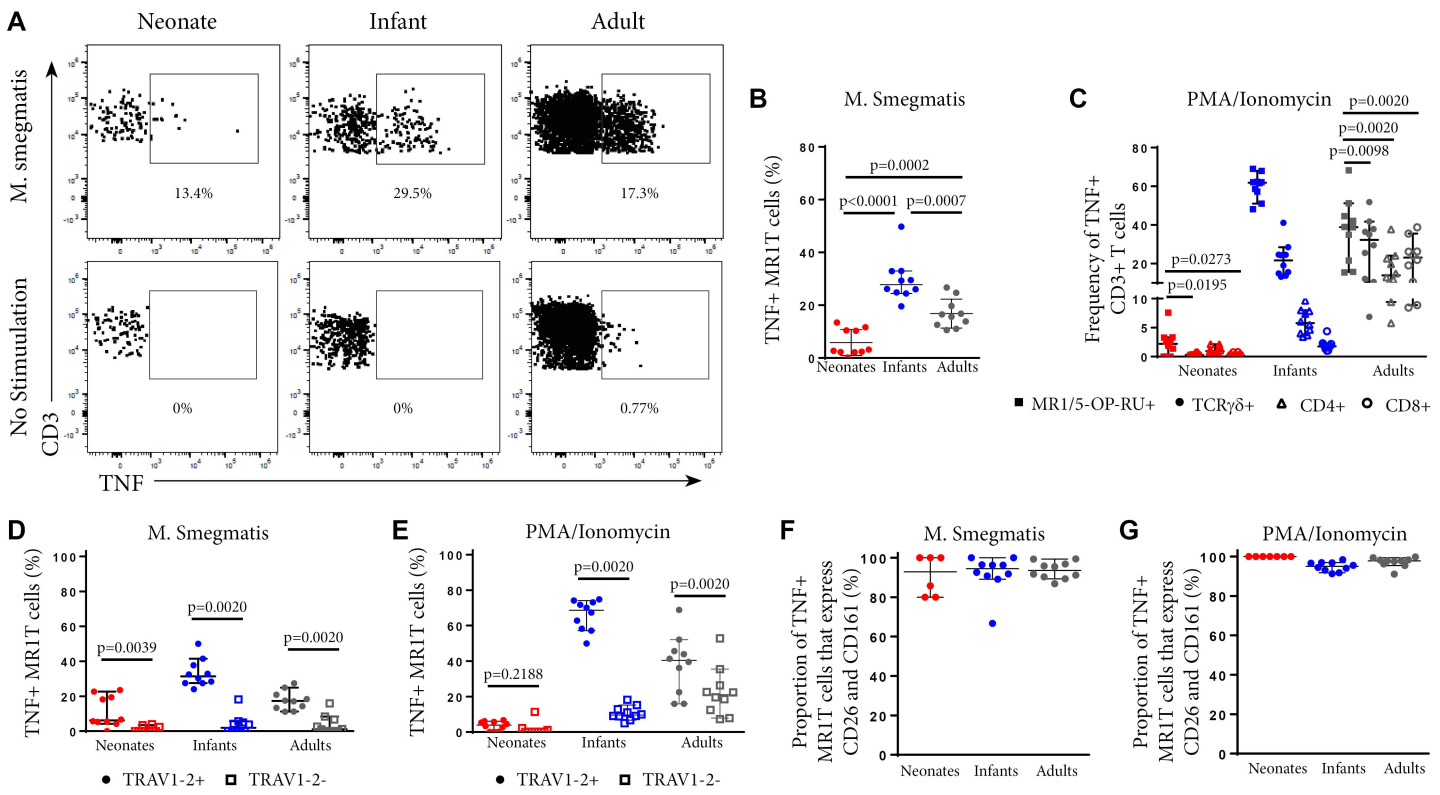
A
Neonate
Infant
Adult
M. smegmatis
No Stimulation
CD3
TNF
13.4%
29.5%
17.3%
0%
0%
0.77%
B
M. Smegmatis
TNF+ MR1T cells (%)
p=0.0002
p<0.0001
p=0.0007
Neonates
Infants
Adults
C
PMA/Ionomycin
Frequency of TNF+ CD3+ T cells
p=0.0020
p=0.0020
p=0.0098
p=0.0273
p=0.0195
Neonates
Infants
Adults
MR1/5-OP-RU+
TCRγδ+
CD4+
CD8+
D
M. Smegmatis
TNF+ MR1T cells (%)
p=0.0039
p=0.0020
p=0.0020
Neonates
Infants
Adults
TRAV1-2+
TRAV1-2-
E
PMA/Ionomycin
TNF+ MR1T cells (%)
p=0.2188
p=0.0020
p=0.0020
Neonates
Infants
Adults
TRAV1-2+
TRAV1-2-
F
M. Smegmatis
Proportion of TNF+ MR1T cells that express CD26 and CD161 (%)
Neonates
Infants
Adults
G
PMA/Ionomycin
Proportion of TNF+ MR1T cells that express CD26 and CD161 (%)
Neonates
Infants
Adults

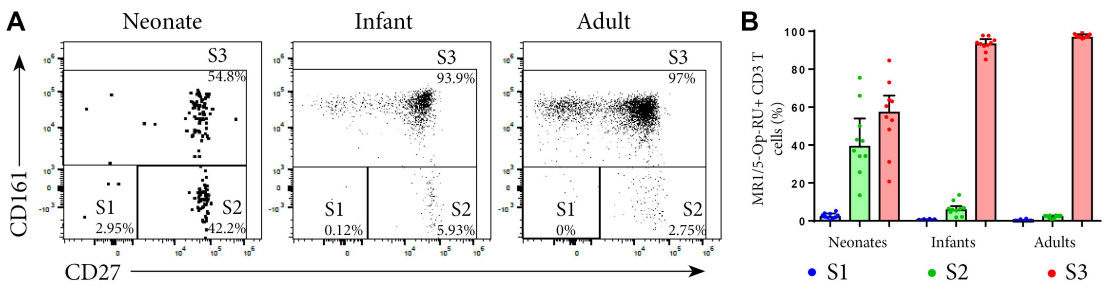
A
Neonate
Infant
Adult
S3
54.8%
S1
2.95%
S2
42.2%
S3
93.9%
S1
0.12%
S2
5.93%
S3
97%
S1
0%
S2
2.75%
CD161
CD27
B
MR1/5-Op-RU+ CD3 T cells (%)
Neonates
Infants
Adults
S1
S2
S3

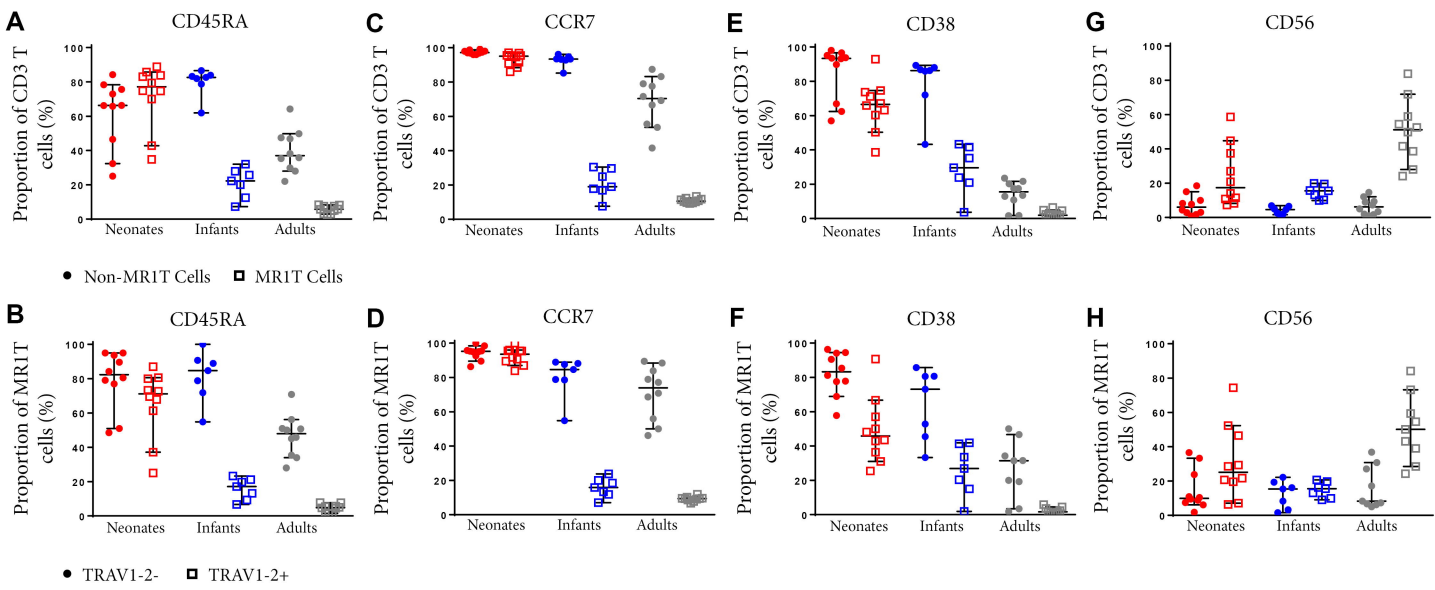
A
CD45RA
Proportion of CD3 T cells (%)
Neonates
Infants
Adults
C
CCR7
E
CD38
G
CD56
Non-MR1T Cells
MR1T Cells
B
CD45RA
Proportion of MR1T cells (%)
D
CCR7
F
CD38
H
CD56
TRAV1-2-
TRAV1-2+